

# Communication with 1-Bit Quantization and Oversampling at the Receiver: Spectral Constrained Waveform Optimization

Sandra Bender, Lukas Landau, Meik Dörpinghaus, and Gerhard Fettweis  
Vodafone Chair Mobile Communication Systems  
Technische Universität Dresden, 01062 Dresden, Germany  
Email: {sandra.bender, lukas.landau, meik.doerpinghaus, fettweis}@tu-dresden.de

**Abstract**—In case of wideband communications the analog-to-digital converter becomes a power consumption implementation bottleneck. Alternatively, transmission schemes based on coarse (1-bit) quantization and oversampling at the receiver can be beneficial. In this regard, information is conveyed in the zero-crossings. However, in presence of spectral constraints the waveform design becomes a challenge. In this work, faster-than-Nyquist BPSK signaling is considered, where runlength limited sequences are applied in order to engineer intersymbol interference. In addition, to further improve the achievable rate, the waveform is optimized by applying a suboptimal design criterion which corresponds to a convex optimization problem. A rate improvement of 10 to 20 percent by optimizing the waveform is observed, in comparison to Gaussian pulses, considering the spectral mask for the IEEE 802.11ad standard. For all cases, the simulation results show that using run-length limited input sequences is superior in terms of achievable rate as compared to independent uniformly distributed input symbols.

## I. INTRODUCTION

The continued demand for faster communication systems is driving data rates well beyond 10Gb/s. E.g., in [1] the scenario of board-to-board communication is investigated, considering data rates of 100 Gbit/s at carrier frequencies in the range between 100-300 GHz. Digitizing the signal with a bandwidth of 10 GHz and beyond imposes challenging requirements on the frontend, namely the analog-to-digital converter (ADC). Surveys, e.g. [2], show that power limited high sampling rates come at the price of coarse quantization. In addition, todays reduced supply voltage of scaled-down CMOS circuits leaves only a small voltage headroom for amplitude processing. But their short switching times make it feasible to increase resolution in time, i.e., processing in time domain [3].

Considering this, using an ADC with coarse (1 bit) quantization can be beneficial as the low resolution can be compensated by higher signaling and sampling rates. This is also in line with two earlier studies. On one hand, Mazo [4] showed rate improvements when applying faster-than-Nyquist signaling (FTN). On the other hand, Shamai [5] showed that for a specific bandlimited process at least

$$I = \log_2(M + 1) \text{ [bits per Nyquist interval]} \quad (1)$$

This work is supported in a part by the German Research Foundation (DFG) in the Collaborative Research Center "Highly Adaptive Energy-Efficient Computing", SFB912, HAEC.

are achievable when sampling the sign  $M$ -times faster than the Nyquist rate. In the present work we apply FTN signaling in combination with  $M$ -fold oversampling at the ADC with respect to the signaling rate under 1-bit quantization at the receiver.

More recently, in [6] it was shown for the low signal-to-noise ratio (SNR) regime, that the capacity per unit-cost can be increased by oversampling w.r.t. Nyquist rate. For the high SNR regime, benefits in terms of achievable rate were shown in [7] due to oversampling. Other studies consider scenarios without hard bandlimitation. For example, [8] and [9] demonstrate that appropriate sequence design based on 4-ASK symbols is beneficial in terms of the achievable rate. Furthermore, binary sequence design and faster-than-Nyquist signaling is considered in [10]. Unlike the aforementioned work, the present investigation considers spectral constraints that are part of almost all wireless communication systems. Therefore the contribution of this work can be summarized as follows

- compliance with a spectral mask according to the IEEE 802.11ad standard is assured,
- it is shown that runlength limited (RLL) sequences are appropriate input sequences in order to resolve the intersymbol interference (ISI) imposed by the spectral constraints and in combination with FTN rates above the intuitive one bit per Nyquist interval for binary inputs can be achieved,
- optimized waveforms provide a further increase in achievable rate and a further rate improvement can be achieved by oversampling w.r.t. the signaling rate.

For the remainder of the paper, the following notation will be applied:  $x_u^l = [x_u, \dots, x_l]^T$  and  $x^l$  for  $u = 1$ , respectively, are sequences of the values of a process  $\{x\}$  from time instant  $u$  to  $l$  while  $x_l$  is the value of  $\{x\}$  at time instant  $l$ . Vectors are denoted by  $\mathbf{y}$  and, equivalently,  $\mathbf{y}_u^l = [\mathbf{y}_u, \dots, \mathbf{y}_l]^T$  and  $\mathbf{y}_l$  refer to sequences and time instances of the corresponding vector, respectively.

## II. SYSTEM MODEL

The considered system model is depicted in Fig. 1. The RLL input sequence consists of input symbols  $x_l$ . RLL sequences have a number of special properties as adjustable robustness

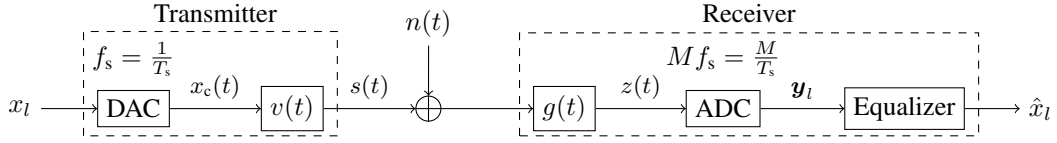


Fig. 1. Continuous time baseband system model

to ISI and spectral characteristics that will be briefly explained in Section III.

The digital input is digital-to-analog converted with the signaling rate  $f_s = \frac{1}{T_s}$  and pulse shaped by the real valued filter  $v(t)$ . Hereby, due to FTN signaling,  $f_s$  can be arbitrarily high as long as the spectral constraints are not violated. The signal  $s(t)$  is then transmitted over the additive white Gaussian noise (AWGN) channel with noise power density  $N_0/2$ . At the receiver the signal is filtered with  $g(t) = v(T_s - t)$ . Then the overall channel impulse response corresponds to the autocorrelation of transmit and receive filter, respectively. Thus while optimizing the overall channel impulse response  $h(t) = v(t) * g(t)$ , the spectral characteristics of  $g(t)$  are known through

$$H(f) = |G(f)|^2. \quad (2)$$

This significantly relieves the complexity of optimization. The received signal is then given by

$$z(t) = \left( \sum_{l=-\infty}^{\infty} x_l \delta(t - lT_s) * v(t) + n(t) \right) * g(t). \quad (3)$$

After filtering, the received signal is passed to the ADC where it is sampled with frequency  $f_{\text{samp}} = Mf_s$ , i.e., oversampled by factor  $M$ . Then, corresponding to every symbol  $x_l$  we get a received vector

$$\mathbf{y}_l = Q_1\{z_l\} = Q_1\{\mathbf{H}\mathbf{U}x_{l-L_{\text{ch}}}^l + \mathbf{G}\mathbf{n}_{l-L_{\text{rx}}}^l\} \quad (4)$$

of length  $M$ , where

$$Q_1\{z_{l,m}\} = \begin{cases} 1, & \text{for } z_{l,m} \geq 0 \\ -1, & \text{otherwise} \end{cases} \quad (5)$$

is the 1-bit quantization function.  $L_{\text{ch}}$  denotes the channel memory introduced by  $h(t)$ , and  $\mathbf{U}$  is the data upsampling matrix of size  $M(L_{\text{ch}} + 2) - 1 \times L_{\text{ch}} + 1$ . Its entries for the  $i$ th row and  $j$ th column are given by

$$U_{i,j} = \begin{cases} 1, & \text{for } i = jM \\ 0, & \text{otherwise} \end{cases}. \quad (6)$$

The vector  $\mathbf{n}_l$  represents the  $M$  samples of the Gaussian white noise.  $L_{\text{rx}} = \frac{L_{\text{ch}}}{2} + 1$ , with  $L_{\text{ch}}$  being even due to the filtering assumed above, is the number of noise vectors to be considered in order to account for the correlation introduced on the noise signal by the receive filter  $g(t)$ .

The filter matrices  $\mathbf{H}$  of size  $M \times M(L_{\text{ch}} + 2) - 1$  and  $\mathbf{G}$  of size  $M \times M(L_{\text{rx}} + 1)$  represent the discrete convolution. Thus, they contain the sampled coefficients of the filters  $h(t)$

and  $g(t)$ , with  $\mathbf{h} = [h_1, h_2, \dots, h_{N_h}]$  and  $\mathbf{g} = [g_1, g_2, \dots, g_{N_g}]$  respectively, and have Toeplitz structure

$$\mathbf{H} = \begin{bmatrix} h_{N_h} & h_{N_h-1} & \dots & h_1 & 0 & 0 & 0 \\ 0 & h_{N_h} & \dots & h_2 & h_1 & 0 & 0 \\ \vdots & \vdots & \ddots & \vdots & \vdots & \vdots & \vdots \\ 0 & 0 & \dots & h_{N_h} & \dots & h_2 & h_1 \end{bmatrix},$$

$$\mathbf{G} = \begin{bmatrix} g_{N_g} & g_{N_g-1} & \dots & g_1 & 0 & 0 & 0 & 0 \\ 0 & g_{N_g} & \dots & g_2 & g_1 & 0 & 0 & 0 \\ \vdots & \vdots & \ddots & \vdots & \vdots & \vdots & \vdots & \vdots \\ 0 & 0 & \dots & g_{N_g} & \dots & g_2 & g_1 & 0 \end{bmatrix},$$

where  $N_h = M(L_{\text{ch}} + 1)$  and  $N_g = ML_{\text{rx}}$  are the lengths of the filters  $\mathbf{h}$  and  $\mathbf{g}$ , respectively. As a result, the noise variance and correlation at the receiver depends on  $v(t)$  with the noise correlation matrix  $\mathbf{R}$  being

$$\mathbf{R} = \sigma_n^2 (\mathbf{G}\mathbf{G}^H) \quad (7)$$

where  $\sigma_n^2$  is the noise energy per sample. At the receiver, perfect synchronization is assumed.

Regarding the spectral constraints it is referred to the established 60 GHz communications. It can be assumed that the basic characteristics of the mask will remain towards for frequencies. We consider the latest IEEE 802.11ad-mask [11]. Its 3 dB-frequency  $f_{3\text{dB,Mask}}$  is 0.98 GHz, which is going to be the reference in terms of bandwidth.

### III. PROPERTIES OF RUNLENGTH LIMITED SEQUENCES

RLL sequences have been widely studied in the field of magnetic and optical recording [12]. The term runlength refers to the number of consecutive alike symbols and is limited by two constraints: a minimum and a maximum runlength, respectively.

The concept of RLL sequences is very closely related to so called  $dk$ -sequences. These are binary sequences where every 1 has to be followed by at least  $d$  and at most  $k$  zeros. The mapping from  $dk$ -sequences to RLL sequences is known as non-return-to-zero-inverse (NRZI) coding, where every one will translate into a zero-crossing. This is illustrated in the following example:

$$\tilde{x} = [\dots 1, 0, 1, 0, 0, 1, 0, 1, \dots] \text{ } dk\text{-seq.}$$

$$x = [\dots 1, 1, -1, -1, -1, 1, 1, -1, \dots] \text{ } \text{RLL seq.}$$

The constraints  $d$  and  $k$  on the  $dk$ -sequences translate into minimum and maximum runlength  $d + 1$  and  $k + 1$ , respectively. This is the key to the tunable ISI robustness of RLL sequences as minimum runlength controls the maximum transition frequency within the signal and, hence,

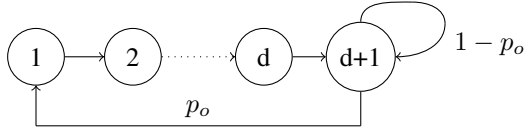


Fig. 2. State diagram of  $d$ -sequence

has an impact on (destructive) ISI when transmitting over a bandlimited channel. For the remainder of this work we consider  $k \rightarrow \infty$ , such that the  $k$ -constraint vanishes. Fig. 2 shows the state diagram of the resulting  $d$ -sequence, where  $p_o$  denotes the probability of the transition back to state one, which results in the occurrence of symbol "one". The capacity of such a sequence can be given by [12]

$$C(d, \infty) = \log_2 \lambda \quad (8)$$

with  $\lambda$  being the largest real root of  $z^{d+1} - z^d - 1 = 0$ . For so called ideal or max-entropic sequences, the  $dk$ -spectrum is given in [12]. For the special case  $k \rightarrow \infty$ , it can be written

$$X(\omega) = \frac{1}{\bar{F} \sin^2\left(\frac{\omega}{2}\right)} \frac{1 - \left| \frac{e^{j(d+1)\omega}}{\lambda^d(\lambda - e^{j\omega})} \right|^2}{\left| 1 + \frac{e^{j(d+1)\omega}}{\lambda^d(\lambda - e^{j\omega})} \right|^2}, \quad (9)$$

where  $\bar{F} = \frac{1}{(\lambda-1)^2} \left( \frac{d+1}{\lambda^{d-1}} - \frac{d}{\lambda^d} \right)$  is the expectation of the runlength. Intuitively,  $X(\omega)$  narrows down with increasing  $d$ . This then impacts the remaining bandwidth for the transmission pulse  $h(t)$ .

#### IV. FILTER DESIGN

##### A. Gaussian Pulses

Simulations with a Gaussian transmission pulse were conducted to obtain general insights on the system performance. Under the consideration of FTN signaling and the spectral constraints, the achievable rate will be defined as

$$I_{\text{ach}} = I_{\text{pcu}} \frac{f_s}{2f_{3\text{dB,Mask}}} \quad [\text{bits per 3dB-interval}], \quad (10)$$

where  $I_{\text{pcu}}$  is the information rate per channel use (pcu), i.e., per  $T_s$ ,  $f_s = \frac{1}{T_s}$  is the signaling rate, and  $f_{3\text{dB,Mask}}$  is the 3dB-frequency of the spectral mask. In Fig. 3 (a)  $I_{\text{pcu}}$  is depicted for different  $d$ - and SNR-values. For very high SNR it can be seen, that until a certain value of  $f_s$  is reached,  $I_{\text{pcu}}$  remains constant at the values  $C(d, \infty)$ . At higher  $f_s$ ,  $I_{\text{pcu}}$  starts to decrease due to longer filter length w.r.t. the symbol duration (and, hence, higher ISI) in order to comply with the spectral mask. It can be concluded that after weighting by  $f_s/2f_{3\text{dB,Mask}}$  said point is the maximum of the achievable rate  $I_{\text{ach}}$ .

It was found that those maxima of  $I_{\text{ach}}$  relate to the filter coefficients of the discrete representation  $\mathbf{h}$  of  $h(t)$ . In the case of the applied binary signaling in order to achieve the input capacity  $C(d, \infty)$ , zero-crossing (ZC) must not be erased. For independent input symbols, this would correspond to evaluating the eye opening of the filter. However, for the RLL-sequences this means, that the filter must be such that a block

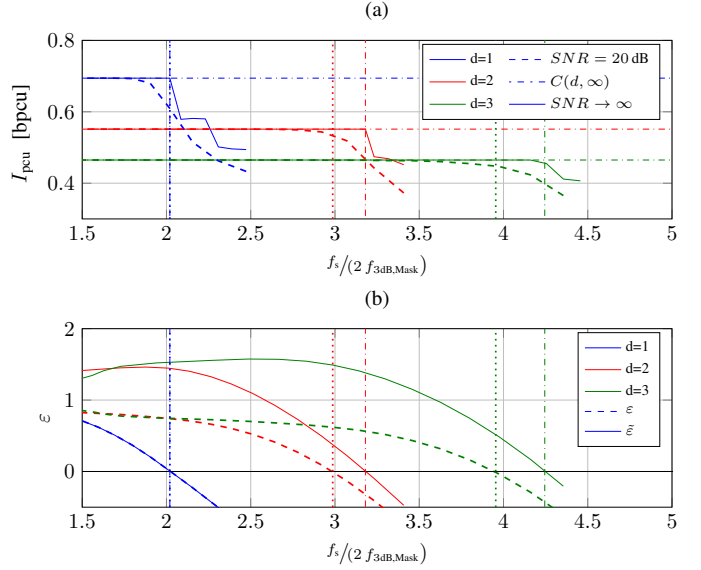


Fig. 3. For a Gaussian filter and  $M = 1$ : (a) information rates pcu for SNR=20dB and very high SNR (SNR  $\rightarrow \infty$ ) and (b) the minimum eye opening  $\varepsilon$  and zero-crossing visibility  $\tilde{\varepsilon}$  of the corresponding filter

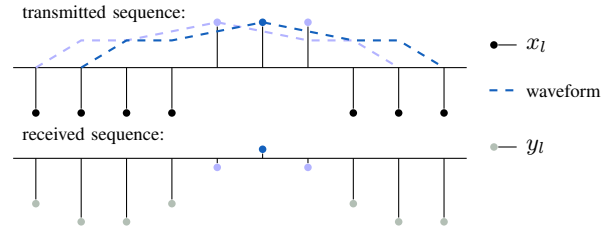


Fig. 4. Example for transmitted and received sequence for  $M = 1$ ,  $d = 2$

of  $d + 1$  consecutive alike symbols cannot be erased. This will be further termed "Visibility of Zero-Crossings". Recall that the filter  $h(t)$  is symmetric. Let  $\mathbf{y}_l$  be the quantized and sampled channel output for an input sequence  $x_{l-i}^{l+i}$  with  $x_l = 1$  and  $i = \frac{L_{\text{ch}}}{2}$ . Then

$$\varepsilon = \min(\mathbf{X} \cdot \mathbf{h}) \quad (11)$$

is half the minimum eye opening for any filter  $h(t)$  with discrete representation  $\mathbf{h}$ . The matrix  $\mathbf{X}$  contains in every line a valid RLL-sequence  $x_{l-i}^{l+i}$  with  $x_l = 1$ . For the visibility of ZC only a subset of  $\mathbf{X}$  has to be considered:  $\tilde{\varepsilon} = \min(\tilde{\mathbf{X}} \cdot \mathbf{h})$ , where  $\tilde{\mathbf{X}}$  contains all RLL input sequences of length  $L_{\text{ch}} + 1$  given (a)  $x_l = 1$  (as before) and (b) the surrounding  $x_{l+j}$  symbols are also equal to 1, with  $j = -\lfloor \frac{d}{2} \rfloor, -\lfloor \frac{d}{2} \rfloor + 1, \dots, \lfloor \frac{d}{2} \rfloor$ .

The difference between both concepts is again illustrated in Fig. 4: For the exemplary filter and  $d = 2$ ,  $\varepsilon < 0$ , i.e. a positive transmitted symbol  $x_l$  can be flipped, which is happening to the light blue symbols in the figure. However, the ZC visibility  $\tilde{\varepsilon} > 0$ , i.e. thanks to the dark blue symbol the receiver still knows that before there has been a sequence of three ones, which is the minimum runlength for  $d = 2$ .

This is confirmed by the second part of the simulation results in Fig. 3 (b), where  $\varepsilon$  and  $\tilde{\varepsilon}$  are depicted. Following

the vertical lines in both parts of the figure, it can be seen for very high SNR: When  $\tilde{\varepsilon} > 0$  also  $I_{\text{pcu}} = C(d, \infty)$  holds. However, this setup is very noise sensitive as can be seen for SNR = 20 dB, where the eye opening  $\varepsilon < 0$  covers better the behaviour of  $I_{\text{pcu}}$ . Hence, if noise resilience is desired, the eye opening is a suitable optimization objective.

### B. Convex Optimization

It can be seen that the filter  $\mathbf{g} = [g_1, g_2, \dots, g_{N_g}]$  of length  $N_g$  with the corresponding transfer function in frequency domain  $G(\omega)$  has to be optimized such that  $|G(\omega)| \leq U(\omega)$ , where the  $U(\omega)$  results from the combination of the spectral mask and the code spectrum of  $x^l$ . This is not necessarily a convex problem, however, Wu and Boyd [13] found that it is possible to solve such kind of problem by replacing the optimization variable  $\mathbf{g}$  by its autocorrelation

$$r_n = \sum_{k=-\infty}^{\infty} g_n g_{n+k}^* \stackrel{(1)}{=} h_n \quad (12)$$

where (1) holds due to Equation (2). This yields always a convex problem

$$\begin{aligned} \text{find} \quad & \mathbf{h} = [h_1, h_2, \dots, h_{N_h}]^T \\ \text{subject to} \quad & 0 \leq H(\omega_i) \leq U^2(\omega_i), \quad \omega_i \in \Omega, \quad i = 1, \dots, m; \end{aligned}$$

where all  $\omega_i$  are equidistantly distributed over the frequency range of interest  $\Omega$ . Due to the method being developed for discrete filters,  $\Omega \subseteq [0, \pi]$ . In order to assure that the full characteristic of the spectral mask can be captured within  $[0, \pi]$ , the resolution during optimization has to be augmented. A resolution grid of  $N_s = 3$  sample points per symbol duration  $T_s$  is chosen.

### C. Waveform Optimization

The eventual goal of the waveform optimization is to maximize or at least increase the information rate. However, it can only be computed numerically for the channel model established in Section II. This prevents us from using the information rate directly as objective regarding the waveform optimization. In Section IV-A, the eye opening has been introduced as suitable optimization objective. Recall that the filter is not discrete but just represented by a set of sampling points according to the oversampled grid  $N_s$ . Due to the oversampling at the receiver,  $M$  of said  $N_s$  filter samples per symbol are of interest as they contribute to the received signal.

When maximizing  $\varepsilon$  as proposed in Section IV-A, the structure of the input sequence is the main influence factor. The minimum eye opening will be maximized depending on the allowed d-constrained input sequences, such that the optimization problem over  $\mathbf{h}$  from Section IV-B results to

$$\begin{aligned} \text{maximize} \quad & \varepsilon \\ \text{subject to} \quad & 0 \leq H(\omega_i) \leq U^2(\omega_i), \quad \omega_i \in \Omega. \\ & \min(\mathbf{X}\mathbf{h}) \geq \varepsilon \end{aligned} \quad (13)$$

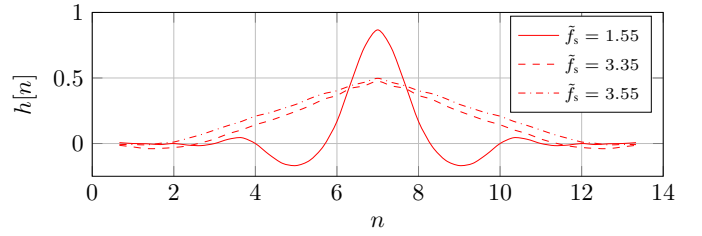


Fig. 5. Optimized pulses for  $M = 1$  ( $\tilde{f}_s = f_s / (2f_{3\text{dB,Mask}})$ )

## V. NUMERICAL EVALUATION

### A. Filter Optimization Results

The optimization was implemented using CVX, a convex optimization toolbox [14]. Thereby, we found that a filter length of  $N_h = 13$  is sufficient for the implementation in terms of a complexity-accuracy-tradeoff. The results are depicted in Fig. 5. It can be observed that with increasing signaling rate, due to the required increase in narrowness in frequency domain, the filter response becomes wider and flatter in time domain. As mentioned before, the computed filter values are calculated on a grid  $\frac{T_s}{N_s}, N_s = 3$ .

### B. Achievable Rate and Bit Error Performance

In order to evaluate the system performance, the achievable rate as stated in Eq. (10) has been chosen as a metric. Simulation-based computation of a lower bound for  $I_{\text{pcu}}$  is applied [15] based on the forward recursion of the BCJR [16] algorithm. It holds

$$\begin{aligned} \lim_{n \rightarrow \infty} \frac{1}{n} I(X^n; \mathbf{Y}^n) \\ \geq -\frac{1}{n} \log_2 W(\mathbf{Y}^n) + \frac{1}{n} \log_2 W(\mathbf{Y}^n | x^n). \end{aligned} \quad (14)$$

The auxiliary channel  $W(\cdot)$  was chosen as proposed in [17]

$$\begin{aligned} \Pr(\mathbf{Y}_l = \mathbf{y}_l | x^l, \mathbf{y}^{l-1}) &\approx \Pr(\mathbf{Y}_l = \mathbf{y}_l | x_{l-L}^l) \\ &= \int_{\mathbb{Y}_i} \frac{1}{2\pi |\mathbf{R}|^{M/2}} \exp\left(-\frac{1}{2} ((z_l - \boldsymbol{\mu}_l) \mathbf{R}^{-1} (z_l - \boldsymbol{\mu}_l)^T)\right) dz_l, \end{aligned} \quad (15)$$

with  $\boldsymbol{\mu}_l = \mathbf{H}\mathbf{U}x_{l-L}^l$  and the quantization region  $\mathbb{Y}_i = \{z_l | Q_1\{z_l\} = \mathbf{y}_i\}$ . The symbol error rate is determined using symbolwise MAP sequence detection. For all simulations, the SNR is defined as

$$\text{SNR} = \frac{\mathbb{E}[s^2(t)]}{N_0 \frac{2f_{3\text{dB,Mask}}}{f_s}}. \quad (16)$$

The high SNR results depicted in Fig. 6 confirm that the application of RLL sequences is superior in terms of maximum achievable rate compared to independent uniformly distributed inputs ( $d=0$ ). This is due to their increased ISI robustness which enables higher  $f_s$  while still achieving  $I_{\text{pcu}} = C(d, \infty)$  despite increased ISI by longer filters. Furthermore, pulse optimization leads to a considerable performance improvement (of 10 to 20 percent) compared to non-optimized pulses. In Fig. 7 it can be seen that the symbol error rate (SER) remains

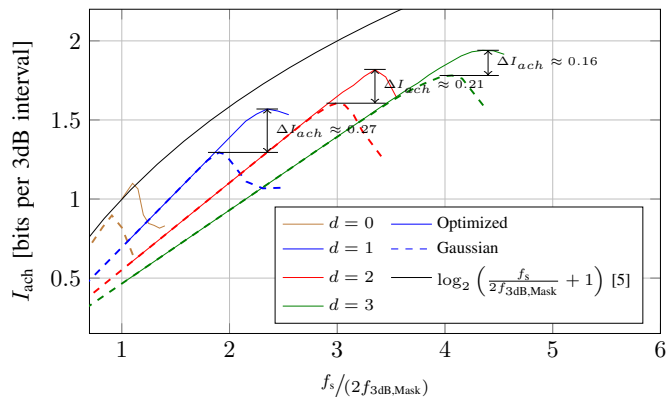


Fig. 6. Achievable rate results for an SNR of 20 dB and  $M = 1$

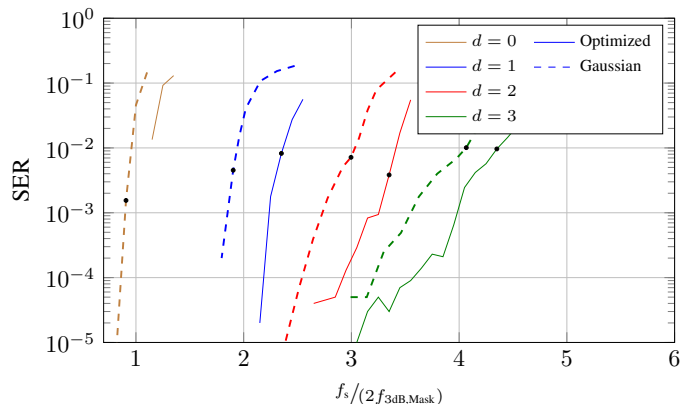


Fig. 7. Symbol error rate results for an SNR of 20 dB and  $M = 1$

roughly stable during optimization (the black dots mark the corresponding rate maximums).

The dependency of the maximum achievable rate on the SNR is depicted in Fig. 8. Exemplarily, the origins of the performance improvements are labeled in the figure. It can be observed that threefold oversampling w.r.t. the signaling rate improves the low SNR performances but has less influence on the high SNR performance. Twofold oversampling was considered as well, however, it leads to sampling at zero-crossings and therefore ambiguities in the BCJR decoder. Furthermore, waveform optimization as well as the combination of RLL input and FTN can produce significant performance increases.

## VI. CONCLUSION

The performance of a spectral constrained AWGN channel and RLL input sequences was considered. It was observed that higher  $d$ -constrained inputs allow for higher signaling rates, which results in an increased achievable rate compared to independent uniformly distributed symbols. It was found that the eye opening is a suitable suboptimal optimization objective for the waveform design which allows for convex optimization. Significant performance improvements (10 to 20 percent) in terms of achievable rate were observed by filter optimization in comparison to Gaussian shaped filtering.

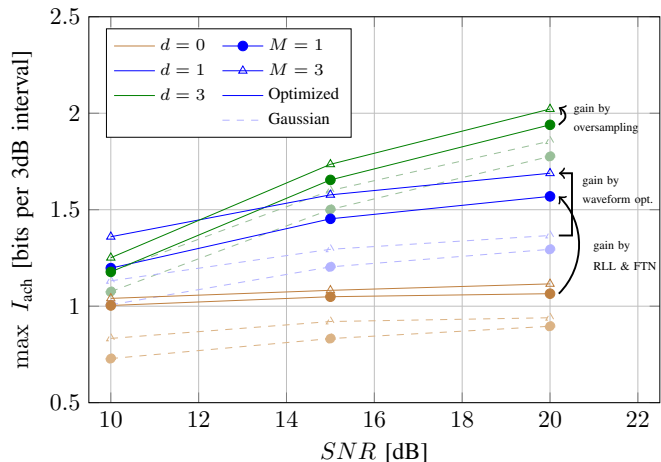


Fig. 8. Achievable rate for different SNR scenarios

## REFERENCES

- [1] G. P. Fettweis, N. ul Hassan, L. Landau, and E. Fischer, "Wireless interconnect for board and chip level," in *Proc. of Design, Automation and Test in Europe (DATE)*, Mar. 2013, pp. 958–963.
- [2] B. Murmann, "ADC Performance Survey 1997-2014." [Online]. Available: <http://www.stanford.edu/~murmann/adcsurvey.html>
- [3] R. Staszewski, "Digitally intensive wireless transceivers," *IEEE Des. Test. Comput.*, vol. 29, no. 6, pp. 7–18, Dec. 2012.
- [4] J. Mazo, "Faster-than-Nyquist signaling," *The Bell System Technical Journal*, vol. 54, p. 14511462, 1975.
- [5] S. Shamai, "Information rates by oversampling the sign of a bandlimited process," *IEEE Trans. Inf. Theory*, vol. 4, no. 4, pp. 1230–1236, 1994.
- [6] T. Koch and A. Lapidith, "Increased capacity per unit-cost by oversampling," in *Proc. of 26th IEEE Convention of Electrical and Electronics Engineers in Israel (IEEEI)*, Nov. 2010, pp. 684–688.
- [7] W. Zhang, "A general framework for transmission with transceiver distortion and some applications," *IEEE Trans. Commun.*, vol. 60, no. 2, pp. 384–399, Feb. 2012.
- [8] T. Hälsig, L. Landau, and G. Fettweis, "Spectral efficient communications employing 1-bit quantization and oversampling at the receiver," in *Proc. of 80th IEEE Vehicular Technology Conference (VTC Fall)*, Sep. 2014, pp. 1–5.
- [9] L. Landau and G. Fettweis, "On reconstructable ask-sequences for receivers employing 1-bit quantization and oversampling," in *Proc. of IEEE International Conference on Ultra-WideBand (ICUWB)*, Sep. 2014, pp. 180–184.
- [10] L. Landau, M. Dörpinghaus, and G. Fettweis, "Communication employing 1-bit quantization and oversampling at the receiver: Faster-than-Nyquist signaling and sequence design," in *Proc. of IEEE International Conference on Ubiquitous Wireless Broadband (ICUWB)*, Oct. 2015.
- [11] Agilent Technologies, "Wireless LAN at 60 GHz - IEEE 802.11ad Explained, Application Note," Tech. Rep., 2013.
- [12] K. Imminck, "Runlength-limited sequences," *Proc. IEEE*, vol. 78, no. 11, pp. 1745–1759, 1990.
- [13] S.-P. Wu, S. Boyd, and L. Vandenberghe, "FIR filter design via semidefinite programming and spectral factorization," in *Proc. of the 35th IEEE Conference on Decision and Control*, vol. 1, Dec. 1996, pp. 271–276.
- [14] M. Grant and S. Boyd, "CVX: Matlab software for disciplined convex programming, version 2.1," <http://cvxr.com/cvx>, Mar. 2014.
- [15] D. Arnold, H.-A. Loeliger, P. Vontobel, A. Kavcic, and W. Zeng, "Simulation-based computation of information rates for channels with memory," *IEEE Trans. Inf. Theory*, vol. 52, no. 8, pp. 3498–3508, 2006.
- [16] L. Bahl, J. Cocke, F. Jelinek, and J. Raviv, "Optimal decoding of linear codes for minimizing symbol error rate," *IEEE Trans. Inf. Theory*, vol. 20, no. 2, pp. 284–287, Mar. 1974.
- [17] L. Landau and G. Fettweis, "Information rates employing 1-bit quantization and oversampling at the receiver," in *Proc. of IEEE 15th International Workshop on Signal Processing Advances in Wireless Communications (SPAWC)*, Jun. 2014, pp. 219–223.